ARTICLE
Journal of Cellular Biochemistry 112:849–859 (2011)

Journal of Cellular Biochemistry

Silybin and Dehydrosilybin Decrease Glucose Uptake by Inhibiting GLUT Proteins

Tianzuo Zhan, Margarete Digel, Eva-Maria Küch, Wolfgang Stremmel, and Joachim Füllekrug*

Molecular Cell Biology Laboratory, Internal Medicine IV, University of Heidelberg, Im Neuenheimer Feld 345, D-69120 Heidelberg, Germany

ABSTRACT

Silybin, the major flavonoid of *Silybum marianum*, is widely used to treat liver diseases such as hepatocellular carcinoma and cirrhosis-associated insulin resistance. Research so far has focused on its anti-oxidant properties. Here, we demonstrate that silybin and its derivative dehydrosilybin inhibit glucose uptake in several model systems. Both flavonoids dose-dependently reduce basal and insulin-dependent glucose uptake of 3T3-L1 adipocytes, with dehydrosilybin showing significantly stronger inhibition. However, insulin signaling was not impaired, and immunofluorescence and subcellular fractionation showed that insulin-induced translocation of GLUT4 to the plasma membrane is also unchanged. Likewise, hexokinase activity was not affected suggesting that silybin and dehydrosilybin interfere directly with glucose transport across the PM. Expression of GLUT4 in CHO cells counteracted the inhibition of glucose uptake by both flavonoids. Moreover, treatment of CHO cells with silybin and dehydrosilybin reduced cell viability which was partially rescued by GLUT4 expression. Kinetic analysis revealed that silybin and dehydrosilybin inhibit GLUT4-mediated glucose transport in a competitive manner with $K_i = 60$ and 116 μM, respectively. We conclude that silybin and dehydrosilybin inhibit cellular glucose uptake by directly interacting with GLUT transporters. Glucose starvation offers a novel explanation for the anti-cancer effects of silybin. J. Cell. Biochem. 112: 849–859, 2011.

KEY WORDS: SILYBIN; INSULIN; DEHYDROSILYBIN; GLUT4; FLAVONOID; 3T3-L1 ADIPOCYTES; GLUCOSE

Glucose metabolism plays a key role in the maintenance of energy homeostasis in organisms and changes in cellular glucose uptake rate are found in many major diseases. A reduced glucose transport into insulin-sensitive tissue is a hallmark of type 2 diabetes. In contrast, a significant increase in glucose consumption can be found in many malignant conditions [Lapela et al., 1995] and during inflammation [Rudd et al., 2002]. The main proteins responsible for glucose influx into cells are transporters of the SLC2 family. The membrane-spanning SLC2 transporters form a substrate-specific pore that facilitates the concentration gradient-driven influx of glucose and other carbohydrates. The GLUT isoforms show a tissue-specific distribution and a distinct affinity for glucose [Uldry and Thorens, 2004]. The function of GLUT proteins is regulated predominantly by a change of subcellular localization. In muscle and adipose tissue, GLUT4 is the most abundant transporter und translocates from intracellular compartments to the plasma membrane (PM) upon insulin stimulation. In contrast, GLUT1, which is responsible for basal glucose uptake in most cells, is found predominantly at the PM.

Flavonoids derived from plants of traditional medicine such as curcumin have received increasing attention in the past decade as new therapeutic approaches for different diseases [Corson and Crews, 2007]. Silybin (SIL), also known as silibinin, is the major active component of silymarin, an extract of the blessed milk thistle *Silybum marianum Gaertneri*, and consists of the diastereomers silybin A and B. *Silybum marianum* has been used in the treatment of liver diseases for two millennia. Several clinical trials have highlighted the beneficial effect of SIL for non-alcoholic fatty liver disease [Federico et al., 2006], chronic hepatitis C infection [Ferenci et al., 2008], and insulin resistance associated with chronic hepatic diseases [Lirussi et al., 2002]. In addition, there is considerable data showing strong inhibitory effects of SIL on the proliferation and survival of different cancer cells in vitro and in vivo [Singh et al., 2008; Garcia-Maceira and Mateo, 2009], leading to clinical trials

Additional supporting information may be found in the online version of this article.

*Correspondence to: Joachim Füllekrug, PhD, Molecular Cell Biology Laboratory, Internal Medicine IV, University of Heidelberg, Im Neuenheimer Feld 345, D-69120 Heidelberg, Germany.
E-mail: joachim.fuellekrug@med.uni-heidelberg.de

Received 4 April 2010; Accepted 25 November 2010 • DOI 10.1002/jcb.22984 • © 2010 Wiley-Liss, Inc.
Published online 7 December 2010 in Wiley Online Library (wileyonlinelibrary.com).

assessing its effectiveness in patients [Singh and Agarwal, 2004]. 2,3-Dehydrosilybin (DHS) is an oxidized form of SIL, occurs naturally in the fruit of the Eurasian spotted milk thistle and is reported to possess stronger anti-oxidant and anti-cancer effects than SIL [Huber et al., 2008]. Most of the biological effects of SIL have been attributed to its anti-oxidant capacity [Mira et al., 1994; Pietrangelo et al., 1995]. However, recent publications indicate a wider range of action, including an inhibition of NF-κB signaling pathway in hepatocytes [Polyak et al., 2007] and of hypoxia-induced factor-α in cancer cells [Garcia-Maceira and Mateo, 2009]. A screen performed by Nomura et al. [2008] identified SIL as an inhibitor of insulin-mediated glucose uptake, but the exact mechanism of this inhibitory effect was not completely resolved. Since changes in glucose metabolism are found in many diseases for which SIL is an effective treatment, including insulin resistance and cancer, we investigated the effect of SIL and DHS on glucose uptake. Our results show that SIL and DHS inhibit cellular glucose uptake by a direct interaction with GLUT4 rather than an interference with insulin signaling or GLUT4 translocation. This reduced availability of glucose is a novel explanation for the anti-cancer effects of SIL.

MATERIALS AND METHODS

ANTIBODIES AND REAGENTS

Silybin (silybin A and B; Sigma S0417, Deisenhofen, Germany) was dissolved in DMSO at 100 mM and appropriately diluted from this stock solution. Glucose-6-phosphate dehydrogenase (*S. cerevisiae*) and wortmannin were also from Sigma. Dehydrosilybin (DHS) was kindly provided by W. Chamulitrat [Huber et al., 2008]. 2-Deoxy-D-[^{3}H]-glucose was obtained from PerkinElmer (Waltham, MA) and human recombinant insulin from Invitrogen (Karlsruhe, Germany). Mouse polyclonal anti-GLUT4 and rabbit anti-caveolin-1 antibodies were from Santa Cruz Biotechnologies (Heidelberg, Germany) and mouse anti-c-myc antibodies from 9E10 hybridoma supernatant. Mouse anti-Akt (pan), mouse anti-phospho-Akt (Ser473), rabbit anti-AS160 and rabbit anti-pAS160 antibodies were from Cell Signaling Technologies (Danvers, MA). Horseradish peroxidase- and fluorochrome-conjugated secondary antibodies were from Jackson Immunoresearch Laboratories (Westgrove, PA).

CELL LINES AND CULTURE

3T3-L1 fibroblasts from ATCC (CL-173) were cultured in Dulbecco's modified Eagle's medium with 4.5 g/L glucose (Invitrogen), 10% fetal calf serum (Biochrom, Germany), 8 mg/L pantothenic acid, 8 mg/L D-biotin, 100 U ml^{-1} penicillin/streptomycin and 1% GlutaMax (Invitrogen).

CHO-K1 cells were cultured in modified Eagle medium (α-MEM, Invitrogen) with 10% fetal calf serum (Invitrogen), 100 U ml^{-1} penicillin/streptomycin and 1% GlutaMax.

Phoenix-gp cells were cultured in DMEM with 4.5 g/L glucose, 10% fetal calf serum (Invitrogen), 100 U ml^{-1} penicillin/streptomycin and 1% GlutaMax (Invitrogen).

ADIPOCYTE DIFFERENTIATION

3T3-L1 fibroblasts were differentiated as described previously [Kuerschner et al., 2008]. In brief, differentiation was induced in post-confluent 3T3-L1 fibroblasts with medium containing 500 μM 3-isobutyl-1-methylxanthine, 5 μM dexamethasone and 5 μg ml^{-1} insulin (day 0). On days 2–3, the medium was replaced by fresh medium containing 5 μg ml^{-1} insulin. After days 5–6, the medium was replaced every 2 days with fresh standard medium until maturation. Adipocytes were used 8–12 days post-induction for experiments.

2-DEOXYGLUCOSE UPTAKE

Differentiated 3T3-L1 adipocytes, fibroblasts, or CHO cells were starved for 3 h in serum-free medium containing 1% bovine serum albumin (BSA). The cells were then washed and, if indicated, stimulated with 100 ng ml^{-1} insulin together with or without different concentrations of flavonoids in Krebs Ringer HEPES (KRH) buffer (120 mM NaCl, 4.7 mM KCl, 2.2 mM $CaCl_2$, 10 mM HEPES, 1.2 mM KH_2PO_4, 1.2 mM $MgSO_4$, pH 7.4) for 20 min at 37°C. Glucose transport was measured by the addition of [^{3}H]-2-deoxy-D-glucose (final concentration: 0.1 mM 2-deoxy-D-glucose [DOG], 1 μCi ml^{-1}) for 1 or 10 min at 37°C. Uptake was stopped by immediately removing the labeling mix and washing the cells four times with ice-cold phosphate-buffered saline (PBS). The cells were then lysed with 1 M NaOH and an aliquot of each lysate was used for scintillation counting in a Beta-Counter LS 6500 (Beckman-Coulter, CA). Unspecific uptake was measured in the presence of 5 μM cytochalasin B. Results were normalized for protein content measured by Bradford assay.

GENERATION OF STABLY EXPRESSING CELLS

Phoenix gp packaging cells grown on collagen-coated Petri dishes (Ø10 cm) were transfected with the pB.GLUT4.myc7.GFP plasmid [Bogan et al., 2001] or pB.GFP control plasmid using the calcium phosphate precipitation method [Schuck et al., 2004]. Media containing recombinant retroviruses were harvested every 24 h, up to 6 days after transfection, and used to infect dividing 3T3-L1 fibroblasts or CHO-K1 cells. Populations of stably expressing cells were isolated by detecting GFP expression with flow cytometry and subsequent sorting of cells.

IMMUNOFLUORESCENCE

3T3-L1 adipocytes and CHO cells expressing the GLUT4 reporter were grown on coverslips, starved for 3 h in serum-free medium and stimulated with 1 μg ml^{-1} insulin and 40 μM flavonoids for 30 min in KRH buffer. For staining of the externalized myc-epitope, cells were incubated with mouse anti-c-myc-antibody for 1 h at 4°C prior to fixation with 4% paraformaldehyde (PFA). After blocking with PBS containing 1% BSA and 0.5% gelatin, cells were stained with anti-mouse-Cy3 secondary antibody for 1 h at room temperature or overnight at 4°C. The coverslips were mounted using Mowiol (Calbiochem, Germany). Images were acquired on an Olympus IX50 microscope and arranged with Adobe Photoshop (Adobe Systems, CA).

HEXOKINASE ACTIVITY ASSAY

Cell lysates for hexokinase activity assays were prepared as described previously [Robey et al., 1999]. For treatment of cells with indicated substances, 3T3-L1 adipocytes grown on six-well

plates were starved for 3 h in serum-free medium and stimulated for 20 min. Cells were harvested by gently scraping in 400 μl of ice-cold lysis buffer (900 mM KCl, 20 mM $MgCl_2$, 10 mM EDTA, 11.1 mM monothioglycerol, 0.25% Triton X-100, 10 mM glucose, and 20 mM Tris–HCl, pH 8.1) per well, transferred to a reaction tube and incubated for 30 min on ice. The lysates were centrifuged for 5 min at 12,000*g*, 4°C. Aliquots of the resulting supernatant were used for the determination of total hexokinase activity. For direct treatment of cell lysates with SIL or DHS, adipocytes were collected immediately in lysis buffer after starvation and supernatants were incubated for 10 min with 40 μM flavonoids prior to measuring hexokinase activity.

The hexokinase activity was measured using a glucose-6-phosphate-dehydrogenase (G6PDH)-coupled assay [Robey et al., 1999]. The reduction of NADP was monitored spectrophotometrically at 340 nm in the presence of excess G6PDH, glucose, and ATP. The assays (final concentrations: 1 U ml^{-1} G6PDH, 0.5 mg ml^{-1} NADP, 6.7 mM ATP, 7.7 mM $MgCl_2$, 3.8 mM glucose, 45 mM KCl, 1 mM NaH_2PO_4, 10.6 mM monothioglycerol, 0.01% Triton X-100, 0.5 mM EDTA, and 42 mM Tris–HCl, pH 8.5) were performed at room temperature and NADPH formation was measured after 10 min. For direct treatment of lysates, flavonoids were added to the assay mix to a final concentration of 40 μM. The enzyme activity was determined from the regression curve and normalized for protein content using the BCA method.

SUBCELLULAR FRACTIONATION

Subcellular fractionation of 3T3-L1 adipocytes was essentially as described previously [Joost and Schurmann, 2001]. Adipocytes (four 10 cm diameter Petri dishes per condition) were starved in serum-free medium and incubated with the indicated substances for 30 min. After washing three times with ice-cold HES buffer (20 mM HEPES, 1 mM EDTA, 255 mM sucrose, pH 7.4), the cells were collected by scraping in HES buffer containing protease inhibitors (1 mM phenylmethylsulfonyl fluoride, 10 μg ml^{-1} pepstatin, 10 μg ml^{-1} aprotinin, 5 μg ml^{-1} leupeptin) and homogenized by passing through a 22 gauge needle ten times. All following steps were performed at 4°C. The homogenate was centrifuged at 16,000*g* in a F34-6-38 rotor (Eppendorff, Germany) for 30 min. The supernatant of this step was recentrifuged in a Ti70 rotor (Beckman-Coulter, Germany) at 41,000*g* for 20 min. The yielded pellet was designated the high-density membrane (HDM) fraction and the supernatant was centrifuged at 180,000*g* in a Ti70 rotor for 75 min. This resulted in the pellet containing the low-density membrane (LDM) fraction. The pellet from the initial centrifugation at 16,000*g* was resuspended in HES puffer and centrifuged again at 16,000*g* in a F34-6-38 rotor for 30 min. The resulting pellet was resuspended in HES and layered on top of a sucrose cushion (38.5% sucrose, 20 mM HEPES, 1 mM EDTA, pH 7) and centrifuged in a SW41 swing-out rotor (Beckman-Coulter, Germany) at 100,000*g* for 60 min. The interface containing the PM fraction was carefully removed, resuspended in HES, and centrifuged in a Ti70 rotor at 40,000*g* for 20 min, yielding the PM fraction. All pellets were resuspended in sample buffer (62 mM Tris–HCl, pH 6.8, 2% sodium dodecyl sulfate, 10% [w/v] glycerol, 1% [w/v] β-mercaptoethanol) boiled for 5 min at 95°C and stored at −20°C. Total protein of each sample was measured by the BCA method. Immunoblotting was performed with primary antibodies against GLUT4 and caveolin-1 was used as loading control.

WESTERN BLOT ANALYSIS

Equal amounts of protein from either cell lysates (12 μg for determination of Akt) or membrane fractions (18 μg for LDM fraction and 25 μg for PM fraction) were loaded and separated on an 8% SDS–polyacrylamide gel. After electrophoresis, proteins were transferred to nitrocellulose membranes. Equal loading and transfer of samples were verified by Ponceau staining. The membranes were blocked in 5% milk powder in TBS-Tween (50 mM Tris–HCl, pH 7.4, 138 mM NaCl, 2.7 KCl, 0.1% Tween-20) for 30 min and then incubated with primary antibodies in blocking buffer containing either 5% milk powder or 5% BSA. The membranes were then washed, incubated with horseradish peroxidase-conjugated secondary antibodies and the reaction was detected with an enhanced chemiluminescence system (Amersham Life Science, Buckinghamshire, UK).

CYTOTOXICITY ASSAY

The MTT (3-(4,5-dimethylthiazol-2-yl)-2,5-diphenyltetrazolium bromide) assay was performed to determine cytotoxicity [Wang et al., 2008]. CHO cells or 3T3-L1 fibroblasts were seeded into 96-well microtiter plates at a density of 3×10^3 cells/well. After 24 h, the medium was replaced by 100 μl of fresh medium containing serial dilutions of SIL or DHS ($0 - 80$ μM). The cells were then incubated for 20 h, after which 20 μl of MTT solution (5 mg ml^{-1} in PBS, Sigma, Germany) was added to each well. Unreacted dye was removed after 4 h of incubation, the formazan crystals were dissolved in DMSO (200 μl/well) and measured spectrophotometrically at 595 nm. Cell viability was defined relative to untreated control (A_{595nm}[flavonoid] − A_{595nm}[blank]/A_{595nm}[control] − A_{595nm}[blank] × 100%).

STATISTICAL ANALYSIS

Unless otherwise stated, results are expressed as mean ± standard error of the mean of at least three independent experiments. Differences between multiple groups were analyzed using one-way ANOVA. Post-ANOVA analysis was performed using Bonferroni's multiple-range *t*-test and $P < 0.05$ was accepted as statistically significant. Differences between two groups were analyzed using Student's *t*-test and $P < 0.05$ was accepted as statistically significant.

RESULTS

SIL AND DHS INHIBIT BASAL AND INSULIN-STIMULATED GLUCOSE UPTAKE

3T3-L1 cells are a common model for studying glucose transport and can be efficiently differentiated into adipocytes. The rate of basal glucose uptake in 3T3-L1 cells depends on GLUT1, which is predominantly found in the PM [Harrison et al., 1990]. Based on reports that SIL reduces blood glucose levels in diabetic patients [Lirussi et al., 2002; Federico et al., 2006], we initially assumed that SIL and DHS would increase basal glucose uptake in 3T3-L1 cells.

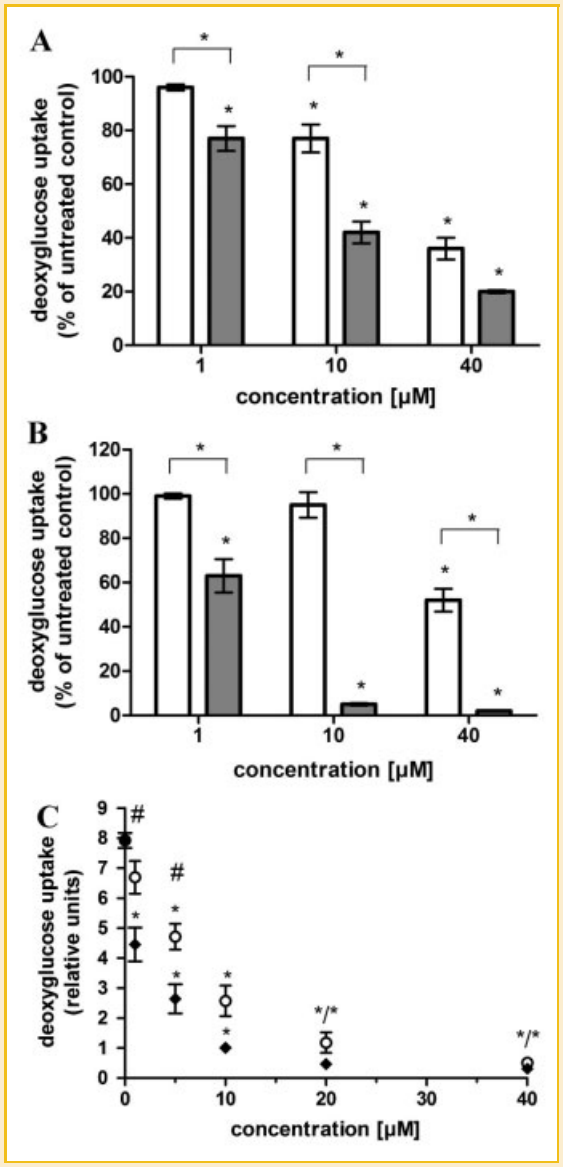

Fig. 1. SIL and DHS inhibit basal and insulin-stimulated glucose uptake. A,B: SIL and DHS dose-dependently reduce basal uptake in 3T3-L1 (A) adipocytes and (B) fibroblasts. 3T3-L1 cells were starved for 3 h in serum-free medium with 1% BSA and incubated for 20 min with different concentrations of SIL (white bars) and DHS (gray bars) in KRH buffer. Labeling mix containing 100 μM ^{3}H-2-DOG (10 Ci mol^{-1}) was added and uptake measured after 10 min. $^{*}P < 0.05$ versus untreated value or between SIL and DHS. C: SIL and DHS dose-dependently reduce insulin-stimulated glucose transport. 3T3-L1 adipocytes were co-incubated with 100 ng ml^{-1} insulin and different concentrations of SIL (white circles) or DHS (black diamonds) for 20 min and then assayed for glucose uptake. The data are presented as relative uptake rates compared to the control (ctrl; no insulin and flavonoids). $^{*}P < 0.05$ versus insulin stimulation. $^{\#}P < 0.05$ between SIL and DHS.

However, adipocytes and fibroblasts treated with SIL and DHS for 20 min showed a strong dose-dependent *decrease* of basal glucose uptake (Fig. 1A,B). This effect was more pronounced for DHS than SIL in both states of differentiation (52% and 36% of control for 40 μM SIL, 5% and 20% of control for 40 μM DHS in fibroblasts and adipocytes, respectively). Next, we investigated the effect of SIL and DHS on insulin-stimulated glucose uptake in adipocytes, which is mainly mediated by GLUT4 [Suzuki and Kono, 1980]. Incubation with 100 ng ml^{-1} insulin resulted in an eightfold increase in glucose uptake, but co-incubation of insulin with different concentrations of SIL or DHS for 20 min dose-dependently reduced glucose influx (Fig. 1C). The effect of insulin on glucose transport was completely abolished at concentrations of 10 μM (DHS) and 20 μM (SIL). These results demonstrate that both flavonoids are strong inhibitors of basal and insulin-stimulated glucose uptake.

SIL AND DHS DO NOT AFFECT INSULIN-DEPENDENT AKT AND AS160 PHOSPHORYLATION

Binding of insulin activates the intrinsic tyrosine kinase activity of the insulin receptor, which initiates a complex signaling cascade resulting in the translocation of GLUT4 to the PM. Within this cascade, the phosphoinositide 3-kinase (PI3K) mediated phosphorylation of the protein kinase Akt and the subsequent phosphorylation of AS160 by phospho-Akt are essential steps [Saltiel and Kahn, 2001]. As SIL was reported to be an inhibitor of Akt phosphorylation in cancer cells [Singh et al., 2008], we investigated the effect of SIL and DHS on insulin-dependent Akt and AS160 phosphorylation.

First, a time course experiment characterized the inhibitory effect of both flavonoids in relation to their incubation time. We pre-incubated adipocytes with insulin and added SIL and DHS at different time points prior to measuring glucose uptake. Increasing pre-incubation periods with insulin and concomitantly decreasing co-incubation periods with flavonoids reduced the inhibitory effect. However, glucose uptake is inhibited even by very short incubation periods (2.5 min), demonstrating that the effects occur almost immediately (Fig. 2A). A comparison with the potent PI3-kinase inhibitor wortmannin shows that SIL and DHS could significantly reduce glucose uptake without any pre-treatment (0 min), which was not observed for wortmannin (Fig. 2B). Next, we investigated the effect of SIL, DHS, and wortmannin on the phosphorylation status of downstream targets of PI3K, Akt and AS160. We pre-incubated adipocytes with insulin for 30 min, added the indicated substances for 20 min and then determined the phosphorylation status of both Akt and AS160 as well as the rate of glucose uptake. Insulin caused a strong increase in phosphorylated Akt and AS160 and this effect was completely inhibited by wortmannin (Fig. 2C). In line with this observation, insulin-mediated increase of glucose uptake was abolished by wortmannin. SIL and DHS inhibited glucose uptake to a similar degree as wortmannin, but had no (SIL) or only minor effects (DHS) on Akt and AS160 phosphorylation (Fig. 2C). Altogether, the results suggest that SIL and DHS inhibit glucose uptake independently of Akt and AS160 phosphorylation.

SIL AND DHS DO NOT INTERFERE WITH GLUT4 TRANSLOCATION

Translocation of GLUT4 from intracellular vesicles to the PM is a critical step for insulin-triggered glucose uptake and is mediated by a complex interaction of proteins and cytoskeleton [Bryant et al., 2002]. Since inhibition of GLUT4 translocation can occur independently of insulin signaling [Olson et al., 2001], we investigated whether GLUT4 translocation to the PM is affected.

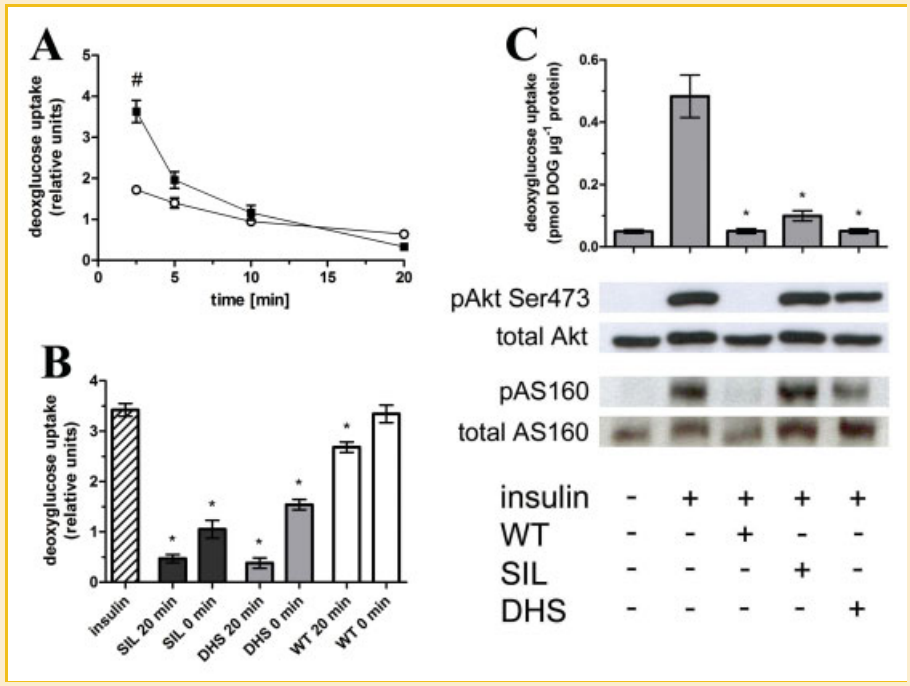

Fig. 2. SIL and DHS do not interfere with insulin-mediated Akt and AS160 phosphorylation. A: SIL- and DHS-mediated inhibition of insulin-stimulated glucose transport is a rapid process. 3T3-L1 adipocytes were starved and incubated with 100 ng ml^{-1} insulin for 30 min. SIL (40 μM; white circles) and DHS (black diamonds) were added at the indicated time points during this incubation prior to measuring glucose uptake. Every value is significantly different from insulin-stimulated cells (sixfold, $P < 0.05$). $^{\#}P < 0.05$ between SIL and DHS. B: The inhibitory capacity of SIL and DHS is different from the PI3-kinase inhibitor wortmannin. 3T3-L1 adipocytes were starved and incubated with 100 ng ml^{-1} insulin for 30 min. SIL (40 μM; dark gray bars), 40 μM DHS (light gray bars) or 100 nM wortmannin (WT) (white bars) were added either 20 min before or together with (0 min) the labeling mix. $^{*}P < 0.05$ versus insulin-stimulated cells. C: SIL has no effect and DHS only a weak effect on insulin-mediated phosphorylation of Akt and AS160. 3T3-L1 adipocytes were starved and pre-incubated with 40 μM SIL/40 μM DHS/100 nM wortmannin, followed by co-incubation with 1 μg/ml insulin for 20 min. The cells were either lysed in sample buffer and incubated with indicated antibodies or assayed for glucose uptake. $^{*}P < 0.05$ versus insulin-stimulated cells without pre-treatment.

We used immunofluorescence microscopy to visualize and quantify the amount of GLUT4 at the PM. First, we stably expressed GLUT4.c-myc7.GFP in 3T3-L1 cells. The GLUT4.c-myc7.GFP reporter construct allows a distinction between total GLUT4 level (GFP) and transporters at the PM (staining of the c-myc-epitope in the first extracellular loop of GLUT4 [Bogan et al., 2001]). Figure 3A shows representative overviews for each condition. Almost no c-myc staining is detectable in the basal state while stimulation with 1 μg ml^{-1} insulin caused a major increase in staining which is not reduced by co-incubation with 40 μM SIL or DHS. We quantified translocation in 3T3-L1 cells based on morphological criteria as done previously by others [Imamura et al., 1999]. Adipocytes were counted on ten randomly selected sites of a coverslip and cells showing distinct c-myc staining of the PM were counted as positive (translocation), while cells with little or no myc staining were counted as negative (no translocation) (Fig. 3B). The number of adipocytes with visible translocation increased ~7-fold under insulin stimulation and was approximately the same when cells were co-incubated with SIL or DHS (Fig. 3C).

We confirmed the results by determining the amount of endogenous GLUT4 at the PM in wild-type 3T3-L1 adipocytes by subcellular fractionation and immunoblotting. At a concentration of 1 μg ml^{-1}, insulin caused an accumulation of GLUT4 in the PM fraction and a parallel reduction in the LDM fraction (Fig. 3D). In line with the results from the previous experiments, co-incubation of insulin with 40 μM SIL or DHS did not change the distribution of GLUT4 in both fractions. Taken together, we applied two independent methods to show that SIL and DHS do not inhibit insulin-induced GLUT4 translocation to the PM.

SIL AND DHS DO NOT REDUCE HEXOKINASE ACTIVITY

The rate of cellular glucose uptake is also determined by hexokinase proteins [Chang et al., 1996]. While GLUT facilitates glucose transport across the PM, the hexokinase phosphorylates intracellular glucose and maintains the concentration gradient required for the influx of glucose. Since SIL and DHS do not inhibit GLUT4 translocation, the next step was to rule out direct inhibitory effects on hexokinases. We measured hexokinase activity in cell lysates from adipocytes that were incubated for 20 min under different conditions by using an enzyme-coupled photometric assay. Neither incubation with 1 μg ml^{-1} insulin alone nor together with SIL or DHS had any significant effect on the hexokinase activity (Fig. 4A). Direct addition of SIL and DHS to cell lysates and the assay mix (final flavonoid concentration 40 μM) did not change hexokinase activity as well (Fig. 4B). Since 2-deoxyglucose is not further metabolized after phosphorylation by the hexokinase, the reduction in glucose uptake is not the result of SIL or DHS targeting further downstream enzymes of glucose metabolism.

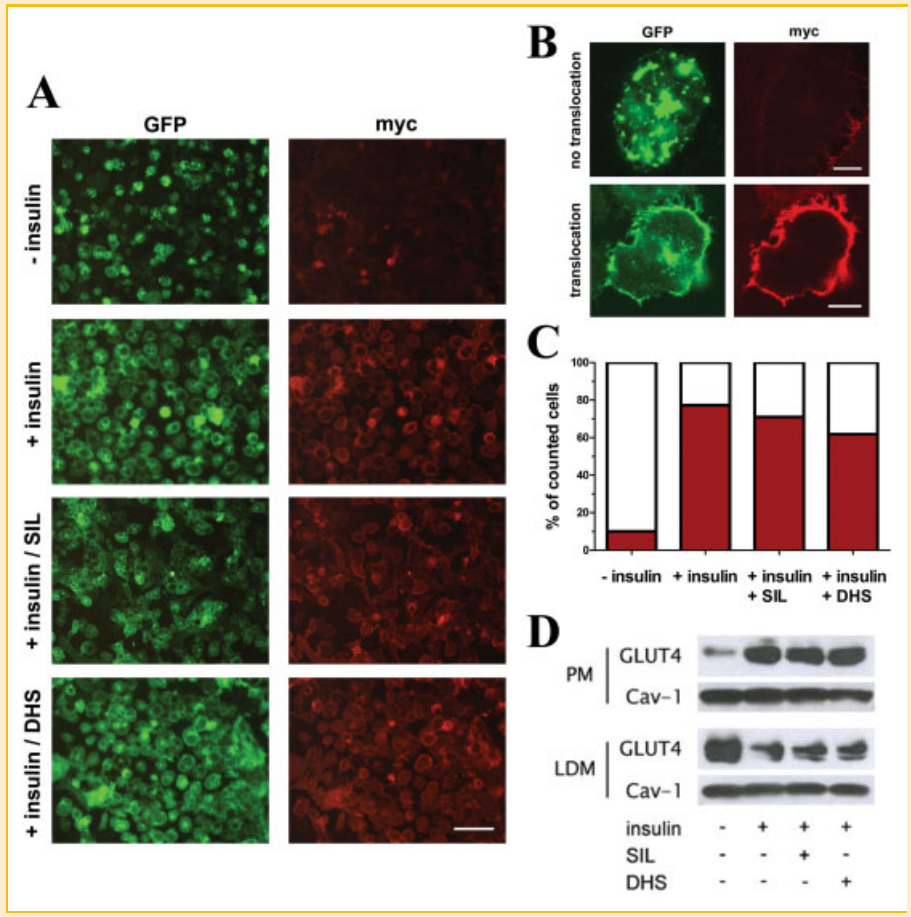

Fig. 3. GLUT4 translocation to the plasma membrane is not inhibited by SIL and DHS. A–C: Insulin-mediated translocation of GLUT4.myc7.GFP is not inhibited by SIL or DHS. 3T3-L1 adipocytes stably expressing GLUT4.c-myc7.GFP were grown on coverslips and starved for 3 h in serum-free medium with 1% BSA. The cells were then stimulated for 30 min with 1 μg ml^{-1} insulin with or without 40 μM flavonoids in KRH buffer, washed and incubated with anti-c-myc antibodies for 1 h at 4°C. They were then fixed with 4% PFA, blocked and incubated overnight with secondary antibodies at 4°C. Overview pictures are shown in (A) and translocation was assessed based on morphological criteria (B). Ten randomly selected pictures were taken for each condition and the number of cells with and without translocation (average of 470 cells per condition) was counted (C). Bars, 100 μm (A) and 10 μm (B). D: Insulin-mediated translocation of GLUT4 in wild-type adipocytes is not inhibited by SIL or DHS. Serum-starved adipocytes were stimulated with 1 μg ml^{-1} insulin with or without 40 μM SIL/DHS for 30 min and fractionated as described under the Materials and Methods Section. Equal amounts of protein were applied, and caveolin-1 (Cav-1) served as a loading control.

EXOGENOUS GLUT4 EXPRESSION IN CHO CELLS REDUCES THE INHIBITORY EFFECT OF SIL AND DHS

Next, we investigated the effect of exogenous GLUT4 expression on the capacity of SIL and DHS to reduce glucose uptake. For this purpose, we heterologously expressed GLUT4.c-myc.GFP in Chinese hamster ovarian (CHO) cells. CHO cells predominantly express GLUT1 as native glucose transporters [Harrison et al., 1991], but have no endogenous GLUT4. Exogenous GLUT4 localizes partially to the PM (Fig. 5A) and increases basal glucose uptake twofold (Fig. 5B). SIL and DHS markedly inhibit basal glucose uptake in CHO cells transfected with the control vector. However, their inhibitory capacity was significantly reduced by GLUT4 expression (Fig. 5B). This result indicates that the level of GLUT4 at the PM is a limiting factor for the inhibitory effect of both flavonoids. In line with previous experiments, the PM localization of GLUT4 is not changed by SIL and DHS (Fig. 5A).

SIL AND DHS COMPETITIVELY INHIBIT GLUCOSE UPTAKE

To further characterize the molecular target of SIL and DHS, we performed a kinetic analysis of their inhibitory effect in insulin-stimulated 3T3-L1 adipocytes. Uptake was determined in the presence of increasing concentrations of deoxyglucose (100, 200, 400, 600 μM) and flavonoids (0, 20, 40, 60 μM). The results were transferred to a Lineweaver-Burk diagram, resulting in a pattern distinct for a competitive inhibitor (Fig. 6). The calculated K_i values were 60 μM for SIL and 114 μM for DHS. As V_{max} is unchanged in competitive inhibition, we performed a statistical analysis to investigate whether the straight lines derived from the four flavonoid concentrations differ significantly in their *y*-axis intersection points. Fitting of results into a linear regression model and subsequent application of an *F*-test shows that the *y*-axis intersection points are not significantly different. GLUT4 mediated glucose uptake is therefore competitively inhibited by SIL and DHS.

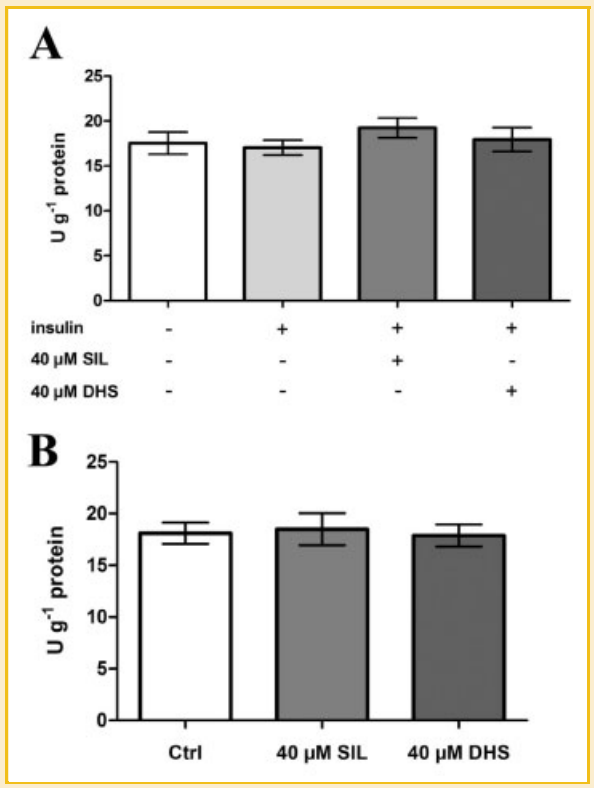

Fig. 4. SIL and DHS do not change hexokinase activity. A,B: Hexokinase activity in 3T3-L1 adipocytes is not changed by SIL or DHS. A: Serum-starved adipocytes were stimulated with 1 µg ml^{-1} insulin with or without 40 µM SIL/DHS, then lysed and assayed for hexokinase activity. B: Lysates of untreated adipocytes were incubated with 40 µM SIL or DHS for 10 min and hexokinase activity was measured in the presence of 40 µM SIL or DHS in the assay mix. Results were obtained from four independent experiments.

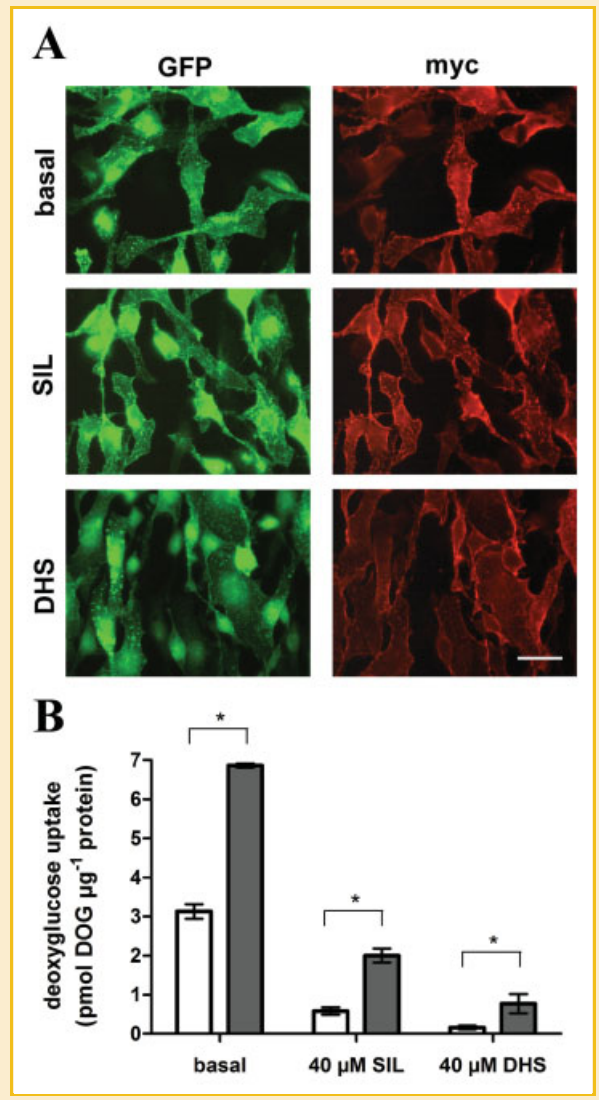

Fig. 5. Expression of GLUT4 in CHO cells reduces the inhibitory effect of SIL and DHS on glucose uptake. A: GLUT4.myc7.GFP expressed in CHO cells localizes partly to the plasma membrane under basal conditions. CHO cells were incubated with anti-c-myc antibodies for 1 h at 4°C, fixed with 4% PFA and incubated with secondary antibodies overnight at 4°C. Bars, 20 µm. B: CHO cells expressing GLUT4.c-myc7.GFP (gray bars) show increased glucose uptake compared to GFP control (white bars). SIL and DHS reduce glucose uptake in control cells, but GLUT4 expression could partially reduce the inhibitory effect. CHO cells were serum-starved for 3 h, incubated with 40 µM SIL or DHS for 20 min and assayed for glucose uptake as described before. *$P < 0.05$ between CHO.GFP and CHO.GLUT4.GFP.

THE CYTOTOXIC EFFECT OF SIL AND DHS IS REDUCED BY GLUT EXPRESSION

SIL and DHS are reported to have cytotoxic effects on different cancer cells lines [Dhanalakshmi et al., 2002; Singh et al., 2008]. As cancer growth is often associated with an increase in glucose consumption, we wanted to investigate whether the cytotoxic effects of SIL and DHS are caused by their inhibition of cellular glucose uptake. Using an MTT assay, we compared the effect of increasing concentrations of SIL and DHS on the viability of CHO cells stably expressing either GLUT4.c-myc7.GFP.pB or GFP.pB. Treatment with SIL or DHS for 24 h caused a dose-dependent reduction of cell viability in GFP expressing cells and this effect was stronger for DHS than SIL (Fig. 7). Expression of GLUT4, however, reduced the cytotoxic effect for SIL and DHS treatment at high flavonoid concentrations. This result suggests that inhibition of glucose uptake is a potential mechanism responsible for the cytotoxic effect of SIL and DHS.

DISCUSSION

Flavonoids are considered as a promising source for drug development and have shown impressing biological effects in vitro and in vivo [Nijveldt et al., 2001]. However, few flavonoid drugs have reached clinical application so far, mostly due to the pleiotropic effects inherent to this class of substances and difficulties to foresee side-effects. SIL is an exception since both its parental extract silymarin and SIL itself (e.g., Legalon SIL®) have been used therapeutically for a long time. Thus, there is considerable amount of data about its efficiency, pharmacokinetics, and safety [Saller et al., 2001]. While the anti-oxidant activity is regarded as the main mechanism underlying the biological effects of SIL for liver diseases,

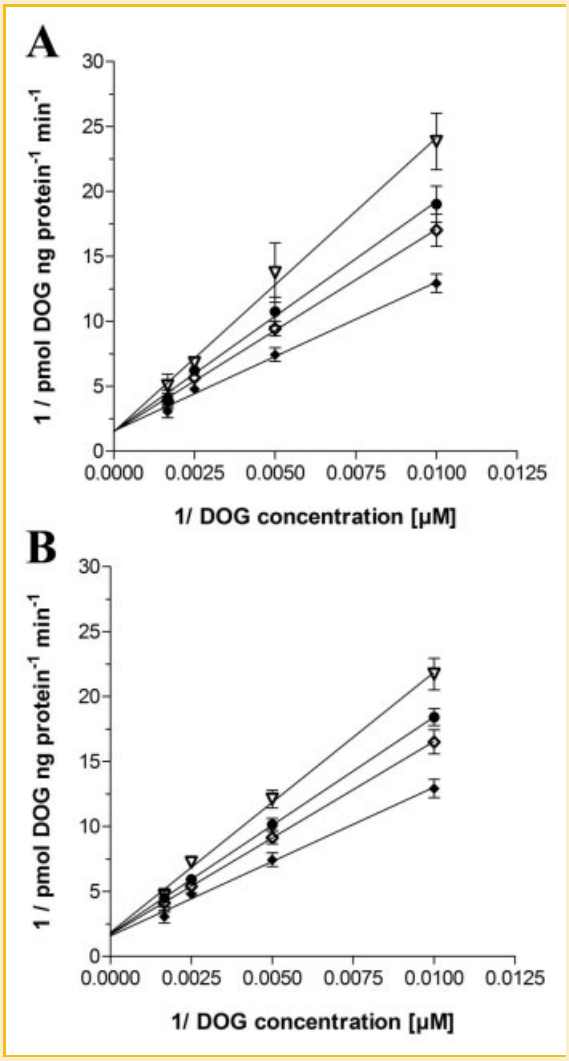

Fig. 6. Competitive inhibition of GLUT4 mediated glucose uptake by SIL and DHS. A,B: Kinetic analysis demonstrates a competitive manner of inhibition for SIL and DHS. Serum-starved adipocytes were stimulated with 100 ng ml^{-1} insulin for 20 min. Labeling mix containing different concentrations of SIL (A) or DHS (B) (0, 20, 40, 60 µM) and deoxyglucose (100, 200, 400, 600 µM) were added for 1 min. Results were plotted on a Lineweaver–Burke diagram. For statistical analysis, a linear regression model was applied, fitting four different regression lines, hereby assuming that the measurement error linearly increases with increasing mean value. A significant difference of *y*-axis intersection points with increasing flavonoid concentrations was not detected by *F*-test ($P = 0.995$ for SIL and $P = 0.864$ for DHS).

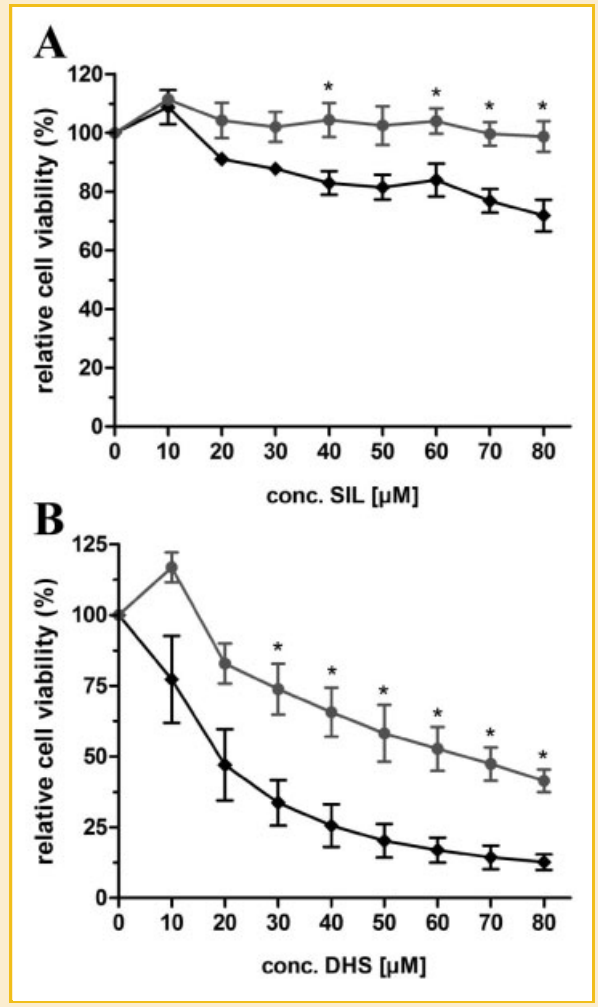

Fig. 7. GLUT4 expression in CHO cells increases resistance to the cytotoxic effects of SIL and DHS. A,B: CHO cells expressing GLUT4.c-myc7.GFP (gray circles) or GFP (black diamonds) were treated with increasing concentrations of SIL (A) or DHS (B) for 24 h. The viability was measured with a MTT assay and the results were obtained from four independent experiments. $^{*}P < 0.05$ between CHO.GFP and CHO.GLUT4.GFP.

more molecular targets have been proposed for its anti-cancer effects [Ramasamy and Agarwal, 2008]. In contrast, little attention was paid to interactions of SIL with glucose metabolism, although severe changes of cellular glucose consumption are found in diseases for which SIL is reported to be beneficial, for example, insulin resistance or cancer.

Our work confirms a previous report showing that SIL can inhibit insulin-stimulated glucose uptake in adipocytes [Nomura et al., 2008]. We investigated the molecular mechanism by which this inhibition is mediated. While the tyrosine kinase activity of the insulin receptor is targeted by a group of flavonoids including genistein [Akiyama et al., 1987], we show that key signaling steps downstream of the insulin receptor including Akt and AS160 phosphorylation are unaffected by SIL. Nomura et al. described that SIL inhibits insulin-mediated translocation of GLUT4. However, we clearly demonstrate that trafficking occurs in spite of SIL and DHS treatment. In addition, we provide evidence that the function of hexokinase, which beside GLUT is the key regulator of glucose uptake, is not compromised. Finally, kinetic analysis of the inhibitory effect demonstrates that both flavonoids reduce GLUT4-mediated glucose transport in a competitive manner. Our results strongly indicate that SIL and DHS share the same binding site as glucose and that they affect glucose uptake by directly reducing glucose binding to GLUT4. In fact, GLUT4 has been described as a structural target of flavonoids that are related to SIL [Strobel et al., 2005]. We could show that basal uptake in 3T3-L1 and CHO cells,

mediated by GLUT1, and in hepatocytes and enterocytes, mediated by GLUT2, is also reduced (Supplement Data). The inhibitory capacity of SIL and DHS is therefore most likely not restricted to GLUT4 but includes other GLUT isoforms. Our results suggest that SIL and DHS have different affinities towards specific GLUT isoforms. While SIL shows higher affinity towards GLUT4, evident in the lower K_i value, DHS is a much stronger inhibitor in cells that predominantly express GLUT2 or GLUT1. However, to clearly identify the individual affinities towards different GLUT isoforms, alternative glucose transport models like *Xenopus laevis* oocytes are required [Nishimura et al., 1993]. An alternative explanation for the inhibitory effect could be an interaction of SIL with the PM leading to conformational changes of GLUT. In fact, SIL was reported to interact with lipid membranes [Wesolowska et al., 2007] and to inhibit other PM bound proteins like multidrug resistance proteins [Lania-Pietrzak et al., 2005]. However, we assume that a hydrophilic rather than hydrophobic site of GLUT is affected by SIL since increasing glucose concentrations can reverse the effect of SIL.

At first sight, our findings seem to contradict reports that show beneficial effects for orally administered SIL on insulin resistance in patients with fatty liver disease [Loguercio et al., 2007]. Reduced glucose uptake into adipocytes is considered a hallmark of insulin resistance and further reduction by SIL would be deleterious rather than beneficial. However, we think that the adipose tissue plays a minor role in the systemic effect of SIL while the liver is predominantly affected. This assumption is based on pharmacokinetic studies showing that oral SIL administration results in plasma peak concentrations of 0.6 μM and biliary concentrations of up to 200 μM [Beckmann-Knopp et al., 2000]. Concentrations of SIL <1 μM have no significant effect on insulin-stimulated glucose uptake in adipocytes (Fig. 1C), whereas concentrations as low as 40 μM can effectively reduce uptake in human hepatic carcinoma cells (Supplement Data). Liver glycogen is synthesized primarily from post-prandial glucose, but also from glucose produced by hepatic gluconeogenesis using amino acids and lipids as substrates [Radziuk and Pye, 2001]. Inhibition of hepatic glucose uptake by SIL would increase the demand for glucose production by gluconeogenesis in order to maintain stable glycogen levels. In patients without severe liver damage and with high body mass index, this could lead to an accelerated turnover of hepatic lipid storages and reduce overt lipid accumulation in the liver [Loguercio et al., 2007]. As fatty liver disease is tightly associated with insulin resistance, the beneficial effect of SIL upon the latter is likely secondary to its effect on the liver. Another mechanism by which SIL may relieve diabetic symptoms is the reduction of intestinal glucose resorption, which was shown for other flavonoids [Kwon et al., 2007]; we also observed this in human colon carcinoma cells (CaCo2; Supplement Data). The situation is more complicated in patients with advanced liver damage, which is the most frequent indication for SIL treatment. Liver cirrhosis is often associated with excessive protein catabolism, malnutrition, and reduced hepatic energy storages [Schuppan and Afdhal, 2008]. A further increase in amino acid mobilization by blocking hepatic glucose uptake would aggravate the pre-existing condition. However, no liver associated complications were observed under SIL treatment. Potential explanations for this discrepancy are complicated by two reasons. First, most clinical studies provide no information on changes of metabolic parameters such as albumin, ammonia level, and body mass index under SIL treatment. Secondly, potential metabolic effects of SIL including adverse effects may be veiled by co-medication, including high-calorie nutritional supplements to reverse protein catabolism [Cabre et al., 1990] or the use of lactulose and antibiotics to reduce ammonia levels. Thus, further studies using amino acid tracers are required to clarify and quantify potential indirect effects of SIL on protein catabolism [Dichi et al., 2001].

Our findings offer a novel explanation for the ability of SIL to reduce proliferation of cancer cells. Research so far has been focusing on the effect of SIL on apoptosis signaling pathways. However, it is well known that many cancer types have an increased glucose turnover and this property is used clinically to localize tumors by FDG-based PET scan [Conti et al., 1996]. The increase of glucose consumption is the result of an overexpression of proteins involved in glucose metabolism, particularly of GLUT1 [Rudlowski et al., 2003]. Elevated levels of GLUT1 in cancer cells correlate significantly with malignancy and reduce metastasis-free survival [Airley et al., 2001]. Therefore, GLUT1 has been proposed as a target for anti-cancer therapy. Using CHO cells, we demonstrated that the cytotoxic effect of SIL and DHS can be partially attributed to their ability to restrict glucose availability by inhibiting GLUT proteins. We confirmed this observation using common cancer cell models including HuH7 and CaCo2 (see Supplement Data). In both cell lines, DHS is a stronger inhibitor of glucose uptake than SIL and this translated into a higher toxicity. These findings support earlier reports showing that inhibition of glucose transport in vitro inhibits proliferation or induces cell death [Rastogi et al., 2007]. However, we think that glucose deprivation is only one of several factors contributing to the anti-tumor effect of SIL and DHS. The relative importance of each factor most likely depends on the flavonoid concentration used and the molecular characteristics of the individual cancer cell lines. Altogether, we show that SIL and DHS would be interesting candidates for an anti-cancer strategy based on reducing glucose supply.

In conclusion, we have demonstrated that silybin, a commonly used flavonoid drug, and its derivative 2,3-dehydrosilybin, are strong inhibitors of glucose uptake in multiple cell lines, including adipocytes and CHO cells. The main molecular mechanism underlying the effect of SIL and DHS on insulin-mediated glucose uptake is not an interference with signaling or GLUT translocation, but a direct competitive inhibition of GLUT4-mediated transport. The reduction in glucose availability caused by SIL and DHS treatment offers a novel alternative explanation for the anti-cancer effects observed for both flavonoids.

ACKNOWLEDGMENTS

We would like to thank Christoph Thiele (MPI Cell Biology and Genetics, Dresden) and Susanne Mandrup (University of Southern Denmark) for helping us to establish the 3T3-L1 cell line, the members of the Söllner group (Biochemistry Center Heidelberg) for continuous technical help, Walee Chamulitrat (Heidelberg University Hospital) for providing silybin/dehydrosilybin, Jonathan S. Bogan (Yale University School of Medicine) for providing the

GLUT4.myc7.GFP.pB plasmid, Dieter Stefan (Institute of Immunology Heidelberg) for helping us with the FACS sorting and Rainer Lüdtke (Karl and Veronica Carstens Foundation) for help with statistical analysis. We also thank Simone Staffer and Sabine Tuma for their excellent technical assistance and Johanna Schott (German Cancer Research Center) for critical comments. The research was supported by the Dietmar Hopp Foundation (to W.S.).

REFERENCES

Airley R, Loncaster J, Davidson S, Bromley M, Roberts S, Patterson A, Hunter R, Stratford I, West C. 2001. Glucose transporter glut-1 expression correlates with tumor hypoxia and predicts metastasis-free survival in advanced carcinoma of the cervix. Clin Cancer Res 7:928–934.

Akiyama T, Ishida J, Nakagawa S, Ogawara H, Watanabe S, Itoh N, Shibuya M, Fukami Y., 1987. Genistein, a specific inhibitor of tyrosine-specific protein kinases. J Biol Chem 262:5592–5595.

Beckmann-Knopp S, Rietbrock S, Weyhenmeyer R, Bocker RH, Beckurts KT, Lang W, Hunz M, Fuhr U. 2000. Inhibitory effects of silibinin on cytochrome P-450 enzymes in human liver microsomes. Pharmacol Toxicol 86:250–256.

Bogan JS, McKee AE, Lodish HF. 2001. Insulin-responsive compartments containing GLUT4 in 3T3-L1 and CHO cells: Regulation by amino acid concentrations. Mol Cell Biol 21:4785–4806.

Bryant NJ, Govers R, James DE. 2002. Regulated transport of the glucose transporter GLUT4. Nat Rev Mol Cell Biol 3:267–277.

Cabre E, Gonzalez-Huix F, Abad-Lacruz A, Esteve M, Acero D, Fernandez-Banares F, Xiol X, Gassull MA. 1990. Effect of total enteral nutrition on the short-term outcome of severely malnourished cirrhotics. A randomized controlled trial. Gastroenterology 98:715–720.

Chang PY, Jensen J, Printz RL, Granner DK, Ivy JL, Moller DE. 1996. Overexpression of hexokinase II in transgenic mice. Evidence that increased phosphorylation augments muscle glucose uptake. J Biol Chem 271:14834–14839.

Conti PS, Lilien DL, Hawley K, Keppler J, Grafton ST, Bading JR. 1996. PET and [18F]-FDG in oncology: A clinical update. Nucl Med Biol 23:717–735.

Corson TW, Crews CM. 2007. Molecular understanding and modern application of traditional medicines: Triumphs and trials. Cell 130:769–774.

Dhanalakshmi S, Singh RP, Agarwal C, Agarwal R. 2002. Silibinin inhibits constitutive and TNFalpha-induced activation of NF-kappaB and sensitizes human prostate carcinoma DU145 cells to TNFalpha-induced apoptosis. Oncogene 21:1759–1767.

Dichi JB, Dichi I, Maio R, Correa CR, Angeleli AY, Bicudo MH, Rezende TA, Burini RC. 2001. Whole-body protein turnover in malnourished patients with child class B and C cirrhosis on diets low to high in protein energy. Nutrition 17:239–242.

Federico A, Trappoliere M, Tuccillo C, de Sio I, Di Leva A, Del Vecchio Blanco C, Loguercio C. 2006. A new silybin-vitamin E-phospholipid complex improves insulin resistance and liver damage in patients with non-alcoholic fatty liver disease: Preliminary observations. Gut 55:901–902.

Ferenci P, Scherzer TM, Kerschner H, Rutter K, Beinhardt S, Hofer H, Schoniger-Hekele M, Holzmann H, Steindl-Munda P. 2008. Silibinin is a potent antiviral agent in patients with chronic hepatitis C not responding to pegylated interferon/ribavirin therapy. Gastroenterology 135(5):1561–1567.

Garcia-Maceira P, Mateo J. 2009. Silibinin inhibits hypoxia-inducible factor-1alpha and mTOR/p70S6K/4E-BP1 signalling pathway in human cervical and hepatoma cancer cells: Implications for anticancer therapy. Oncogene 28:313–324.

Harrison SA, Buxton JM, Clancy BM, Czech MP. 1990. Insulin regulation of hexose transport in mouse 3T3-L1 cells expressing the human HepG2 glucose transporter. J Biol Chem 265:20106–20116.

Harrison SA, Buxton JM, Czech MP. 1991. Suppressed intrinsic catalytic activity of GLUT1 glucose transporters in insulin-sensitive 3T3-L1 adipocytes. Proc Natl Acad Sci USA 88:7839–7843.

Huber A, Thongphasuk P, Erben G, Lehmann WD, Tuma S, Stremmel W, Chamulitrat W. 2008. Significantly greater antioxidant anticancer activities of 2,3-dehydrosilybin than silybin. Biochim Biophys Acta 1780(5):837–847.

Imamura T, Ishibashi K, Dalle S, Ugi S, Olefsky JM. 1999. Endothelin-1-induced GLUT4 translocation is mediated via Galpha(q/11) protein and phosphatidylinositol 3-kinase in 3T3-L1 adipocytes. J Biol Chem 274: 33691–33695.

Joost HG, Schurmann A. 2001. Subcellular fractionation of adipocytes and 3T3-L1 cells. Methods Mol Biol 155:77–82.

Kuerschner L, Moessinger C, Thiele C. 2008. Imaging of lipid biosynthesis: How a neutral lipid enters lipid droplets. Traffic 9:338–352.

Kwon O, Eck P, Chen S, Corpe CP, Lee JH, Kruhlak M, Levine M. 2007. Inhibition of the intestinal glucose transporter GLUT2 by flavonoids. FASEB J 21:366–377.

Lania-Pietrzak B, Michalak K, Hendrich AB, Mosiadz D, Grynkiewicz G, Motohashi N, Shirataki Y. 2005. Modulation of MRP1 protein transport by plant, and synthetically modified flavonoids. Life Sci 77:1879–1891.

Lapela M, Leskinen S, Minn HR, Lindholm P, Klemi PJ, Soderstrom KO, Bergman J, Haaparanta M, Ruotsalainen U, Solin O, Joensuu H. 1995. Increased glucose metabolism in untreated non-Hodgkin's lymphoma: A study with positron emission tomography and fluorine-18-fluorodeoxyglucose. Blood 86:3522–3527.

Lirussi F, Beccarello A, Zanette G, De Monte A, Donadon V, Velussi M, Crepaldi G. 2002. Silybin-beta-cyclodextrin in the treatment of patients with diabetes mellitus and alcoholic liver disease. Efficacy study of a new preparation of an anti-oxidant agent. Diabetes Nutr Metab 15:222–231.

Loguercio C, Federico A, Trappoliere M, Tuccillo C, de Sio I, Di Leva A, Niosi M, D'Auria MV, Capasso R, Del Vecchio Blanco C. 2007. The effect of a silybin-vitamin e-phospholipid complex on nonalcoholic fatty liver disease: A pilot study. Dig Dis Sci 52:2387–2395.

Mira L, Silva M, Manso CF. 1994. Scavenging of reactive oxygen species by silibinin dihemisuccinate. Biochem Pharmacol 48:753–759.

Nijveldt RJ, van Nood E, van Hoorn DE, Boelens PG, van Norren K, van Leeuwen PA. 2001. Flavonoids: A review of probable mechanisms of action and potential applications. Am J Clin Nutr 74:418–425.

Nishimura H, Pallardo FV, Seidner GA, Vannucci S, Simpson IA, Birnbaum MJ. 1993. Kinetics of GLUT1 and GLUT4 glucose transporters expressed in Xenopus oocytes. J Biol Chem 268:8514–8520.

Nomura M, Takahashi T, Nagata N, Tsutsumi K, Kobayashi S, Akiba T, Yokogawa K, Moritani S, Miyamoto K. 2008. Inhibitory mechanisms of flavonoids on insulin-stimulated glucose uptake in MC3T3-G2/PA6 adipose cells. Biol Pharm Bull 31:1403–1409.

Olson AL, Trumbly AR, Gibson GV. 2001. Insulin-mediated GLUT4 translocation is dependent on the microtubule network. J Biol Chem 276:10706–10714.

Pietrangelo A, Borella F, Casalgrandi G, Montosi G, Ceccarelli D, Gallesi D, Giovannini F, Gasparetto A, Masini A. 1995. Antioxidant activity of silybin in vivo during long-term iron overload in rats. Gastroenterology 109:1941–1949.

Polyak SJ, Morishima C, Shuhart MC, Wang CC, Liu Y, Lee DY. 2007. Inhibition of T-cell inflammatory cytokines, hepatocyte NF-kappaB signaling, and HCV infection by standardized Silymarin. Gastroenterology 132:1925–1936.

Radziuk J, Pye S. 2001. Hepatic glucose uptake, gluconeogenesis and the regulation of glycogen synthesis. Diabetes Metab Res Rev 17:250–272.

Ramasamy K, Agarwal R. 2008. Multitargeted therapy of cancer by silymarin. Cancer Lett 269(2):352–362.

Rastogi S, Banerjee S, Chellappan S, Simon GR. 2007. Glut-1 antibodies induce growth arrest and apoptosis in human cancer cell lines. Cancer Lett 257:244–251.

Robey RB, Ma J, Santos AV. 1999. Regulation of mesangial cell hexokinase activity by PKC and the classic MAPK pathway. Am J Physiol 277:F742–F749.

Rudd JH, Warburton EA, Fryer TD, Jones HA, Clark JC, Antoun N, Johnstrom P, Davenport AP, Kirkpatrick PJ, Arch BN, Pickard JD, Weissberg PL. 2002. Imaging atherosclerotic plaque inflammation with [18F]-fluoro-deoxyglucose positron emission tomography. Circulation 105:2708–2711.

Rudlowski C, Becker AJ, Schroder W, Rath W, Buttner R, Moser M. 2003. GLUT1 messenger RNA and protein induction relates to the malignant transformation of cervical cancer. Am J Clin Pathol 120:691–698.

Saller R, Meier R, Brignoli R. 2001. The use of silymarin in the treatment of liver diseases. Drugs 61:2035–2063.

Saltiel AR, Kahn CR. 2001. Insulin signalling and the regulation of glucose and lipid metabolism. Nature 414:799–806.

Schuck S, Manninen A, Honsho M, Fullekrug J, Simons K. 2004. Generation of single and double knockdowns in polarized epithelial cells by retrovirus-mediated RNA interference. Proc Natl Acad Sci USA 101:4912–4917.

Schuppan D, Afdhal NH. 2008. Liver cirrhosis. Lancet 371:838–851.

Singh RP, Agarwal R. 2004. Prostate cancer prevention by silibinin. Curr Cancer Drug Targets 4:1–11.

Singh RP, Gu M, Agarwal R. 2008. Silibinin inhibits colorectal cancer growth by inhibiting tumor cell proliferation and angiogenesis. Cancer Res 68:2043–2050.

Strobel P, Allard C, Perez-Acle T, Calderon R, Aldunate R, Leighton F. 2005. Myricetin, quercetin and catechin-gallate inhibit glucose uptake in isolated rat adipocytes. Biochem J 386:471–478.

Suzuki K, Kono T. 1980. Evidence that insulin causes translocation of glucose transport activity to the plasma membrane from an intracellular storage site. Proc Natl Acad Sci USA 77:2542–2545.

Uldry M, Thorens B. 2004. The SLC2 family of facilitated hexose and polyol transporters. Pflugers Arch 447:480–489.

Wang W, Wu F, Fang F, Tao Y, Yang L. 2008. Inhibition of invasion and metastasis of hepatocellular carcinoma cells via targeting RhoC in vitro and in vivo. Clin Cancer Res 14:6804–6812.

Wesolowska O, Lania-Pietrzak B, Kuzdzal M, Stanczak K, Mosiadz D, Dobryszycki P, Ozyhar A, Komorowska M, Hendrich AB, Michalak K. 2007. Influence of silybin on biophysical properties of phospholipid bilayers. Acta Pharmacol Sin 28:296–306.